Antineoplastic Agents. 410. Asymmetric Hydroxylation of *trans*-Combretastatin A-4[1]

George R. Pettit,*,† Brian E. Toki,† Delbert L. Herald,† Michael R. Boyd,‡ Ernest Hamel,‡ Robin K. Pettit,† and J. Charles Chapuis†

Cancer Research Institute and Department of Chemistry, Arizona State University, P.O. Box 872404, Tempe, Arizona 85287-2404, and Laboratory of Drug Discovery Research and Development, DTP/DCTD, National Cancer Institute, Frederick Cancer Research and Development Center, Frederick, Maryland 21702-1201

Received December 18, 1998

The South African willow tree *Combretum caffrum* has yielded a number of potent cancer cell growth inhibitors. The present SAR studies of the antineoplastic agent combretastatin A-4 (**1c**) were focused mainly on the olefinic bridge to determine the effects on cancer cell growth and, potentially, to better define the combretastatin A-4 binding site on tubulin. The geometric *trans*-isomer **3a** of combretastatin A-4 was converted to the (1*S*,2*S*)- and (1*R*,2*R*)-vicinal diols **4c** and **4d**, respectively, under Sharpless' asymmetric dihydroxylation conditions. Cancer cell line testing showed the (1*S*,2*S*)-diol **4c** to be more potent than its enantiomer **4d**. Diol **4c** weakly inhibited tubulin polymerization (IC_{50} = 22 μM, versus 1.2 μM for combretastatin A-4), while **4d** was inactive (IC_{50} > 40 μM). Esterification of either stereoisomer at the diol and/or phenolic positions resulted in elimination of inhibitory activity.

Introduction

For cancer to progress to metastatic disease, complex biochemical and physiological changes leading to tissue invasion and angiogenesis are required. Such neovascularization is necessary for tumors to grow beyond a spheroid of about 2 mm[3], for diffusion of nutrients cannot support a greater volume of neoplastic cells.[2] Discovery and clinical development of antagonists of such tumor angiogenesis should lead to considerable improvements in cancer treatment.[3,4] Currently some 10 antiangiogenic drugs are in clinical trials, including substances as diverse as thalidomide,[5] a fumagillin derivative (TNP-470),[3,6] and interleukin 12.[3] One of the most promising new antiangiogenic anticancer drugs that began phase I clinical trials in November 1998 is the *cis*-stilbene combretastatin A-4 prodrug (**1a**).[7]

As part of an extensive structure−activity relationship (SAR) study of combretastatin analogues, resulting from our report of the first member of the series (combretastatin, **2a**),[8] we have been evaluating various *trans*-stilbenes[9,10] and their corresponding dihydro derivatives (e.g., **2b**, **2c**). Recently, the *trans*-stilbenes resveratrol[11,12] and 3-hydroxy-4-methoxy-4′-nitro-*trans*-stilbene have been found, respectively, to be chemopreventive[11] and to interfere with the phosphorylation of certain proteins in the B-cell receptor cascade.[13] The current study was directed at ascertaining the effects on cancer cell and microbial growth, inhibition of tubulin polymerization,[14,15] and eventually tumor angiogenesis by the chiral vicinal diols related to combretastatin (**2a**), obtained from the poorly active *trans*-olefin **3a**. Earlier we had synthesized racemic combretastatin (**2a**) as well as isocombretastatin A (**2b**),[8] and that approach was later extended by others[16,17] to related series of compounds.

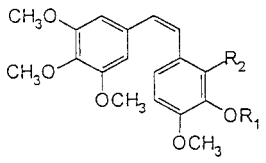

1a, R_1 = PO_3HNa, R_2 = H Combretastatin A-4 prodrug
1b, R_1 = H, R_2 = OH Combretastatin A-1
1c, R_1 = R_2 = H Combretastatin A-4

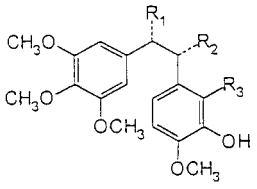

2a, R_1 = OH, R_2 = R_3 = H Combretastatin
2b, R_1 = R_3 = H, R_2 = OH Isocombretastatin A
2c, R_1 = R_2 = H, R_3 = OH Combretastatin B-1

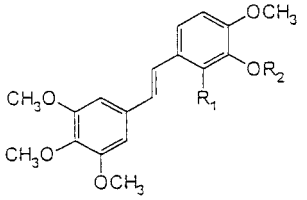

3a, R_1 = R_2 = H
3b, R_1 = OH, R_2 = H
3c, R_1 = H, R_2 = $Si(CH_3)_2C(CH_3)_3$

Our previous studies suggested the need for a *cis*-olefin[18,19] or other sp^2-type[20] unit linking the aryl groups

* To whom correspondence should be addressed.
† Arizona State University.
‡ NCI.

10.1021/jm9807149 CCC: $18.00
Published on Web 04/08/1999

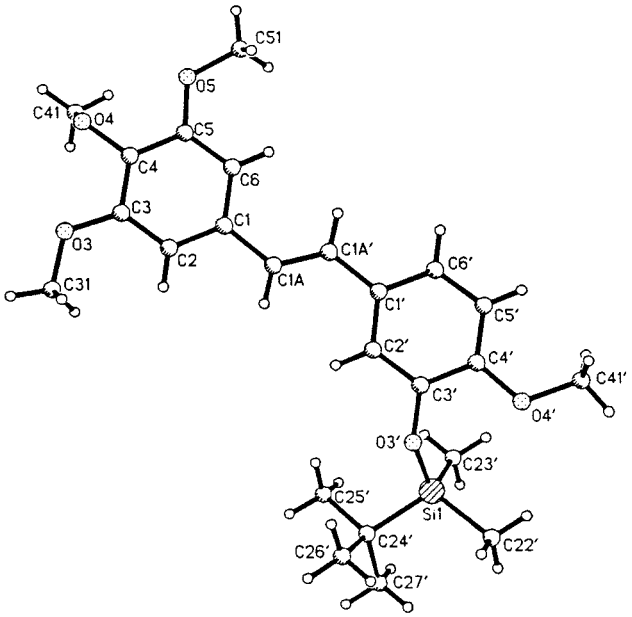

Figure 1. Computer-generated perspective of the silyl ether of the *trans*-stilbene isomer **3c**.

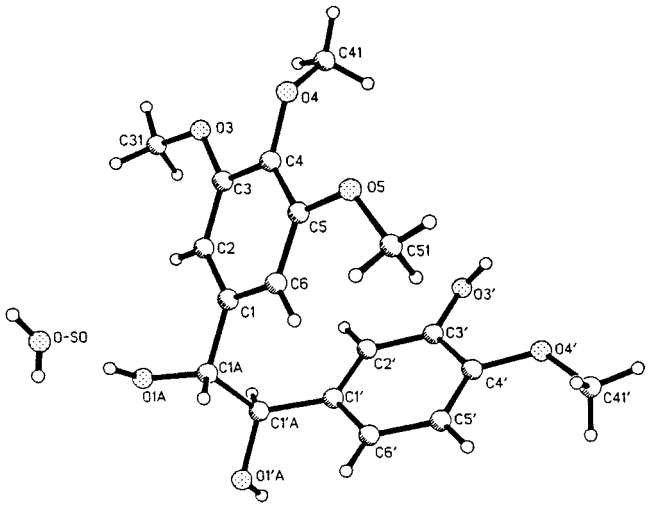

Figure 2. Computer-generated perspective of the ethanediol monohydrate **4d**.

in order to attain high pharmacological activity. Cancer cell line data have clearly shown a progressive decrease in activity with *cis*-stilbenes > 1,2-diphenylethanes > *trans*-stilbenes, as, for example, seen for combretastatin A-1 (**1b**) > combretastatin B-1 (**2c**) > *trans*-isomer of combretastatin A-1 (**3b**).[18] Additional evidence was furnished by the remarkable activity against cancer cell lines of combretastatin A-4 (**1c**) vs its *trans*-isomer. The *Z*-geometry also appears to be quite important for inhibition of tubulin polymerization.

Results and Discussion

Chemistry. The synthesis[18] of combretastatin A-4 (**1c**) was repeated, and the intermediate silyl ether **3c** derivative of **3a** was employed as the starting point for the preparation of the diols. The stereochemistry of the *trans*-isomer **3c** was confirmed by X-ray analysis, and the molecule is shown in Figure 1. The *trans*-isomer **3c** was treated separately with the Sharpless AD mix-α and AD mix-*β* to give the (1*S*,2*S*)- (**4a**) and (1*R*,2*R*)- (**4b**) diols, respectively, as colorless oils (Scheme 1). The reactions were conducted in the dark in order to avoid photochemical isomerization of the double bond. Deprotection using tetrabutylammonium fluoride afforded the phenols **4c** and **4d**. Initial attempts at confirmation of the absolute stereochemistry of the unprotected enantiomers **4c** and **4d**, using X-ray structure determination methods, failed. Although the relative stereochemistry could be readily established via X-ray structure determination, the weak anomalous dispersion exhibited by **4d** (for example) did not allow an unambiguous configurational assignment for this compound (shown in Figure 2) versus that of its enantiomer **4c**. However, the absolute stereochemical assignments of **4c** and **4d**

Scheme 1[a]

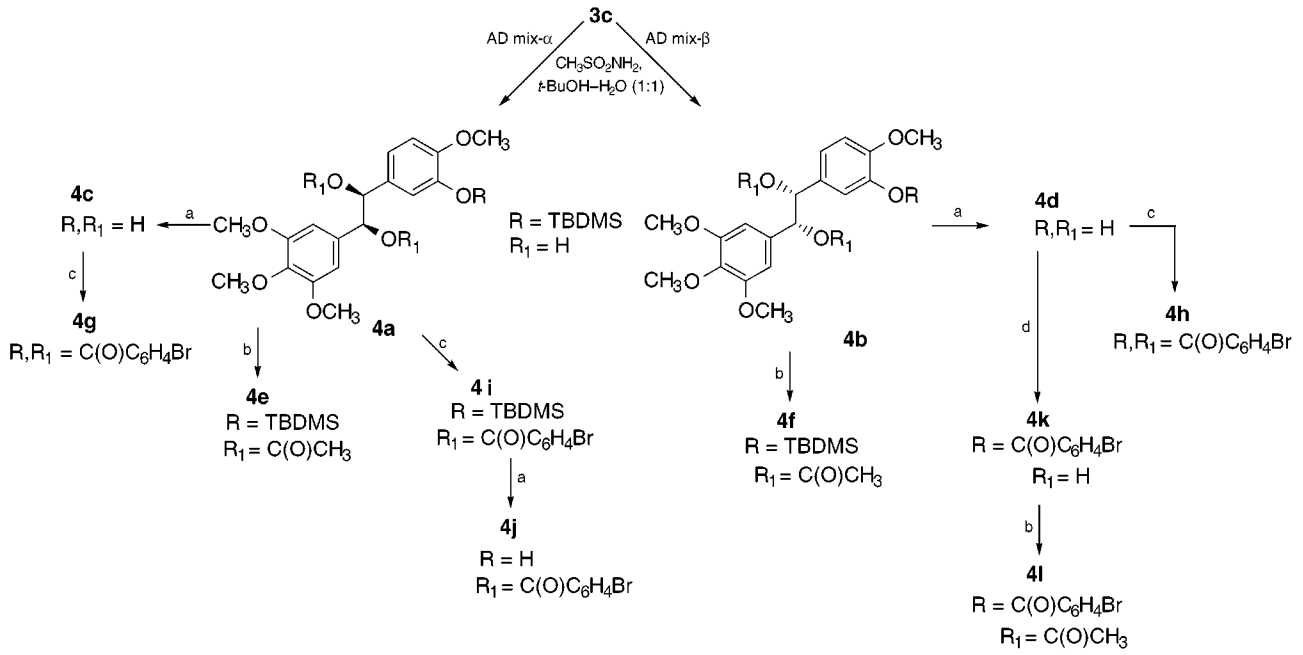

[a] (a) TBAF, THF; (b) Ac_2O, Et_3N, DMAP, DCM; (c) 4-bromobenzoyl chloride, pyridine, DMF; (d) 4-bromobenzoyl chloride, Et_3N, DMF.

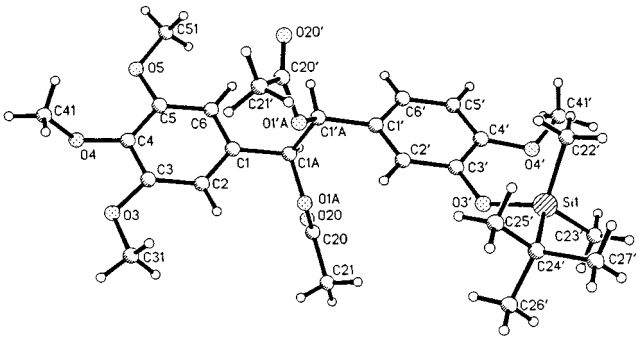

Figure 3. Computer-generated molecular structural drawing of the *tert*-butyldimethylsilyl diacetate derivative **4e**, showing the absolute stereochemistry as *S* at chiral centers C1A and C1′A.

were established by a subsequent X-ray crystal structure determination of one of the enantiomers as the *tert*-butyldimethylsilyl diacetate derivative, i.e., **4e** (Figure 3).

Compound **4e** was prepared by treatment of the TBDMS-protected phenol **4a** with acetic anhydride and triethylamine/DMAP. Thus, the absolute configuration of **4e** (and consequently all compounds derived from **4a**) was established as 1*S*,2*S*. Similarly, the corresponding enantiomers of these compounds derived from **4b** could be assigned the 1*R*,2*R* absolute configuration.

Biological Evaluation. The murine P388 lymphocytic leukemia cell line and human cancer cell line (GI_{50}) data (Table 2) proved to be quite useful. Results of the asymmetric dihydroxylation of *trans*-stilbene **3c** followed by deprotection showed the (1*S*,2*S*)-diol **4c** to be significantly more active than the (1*R*,2*R*)-diol **4d**. The cancer cell growth inhibitory activity was markedly reduced or eliminated by esterifying the hydroxyl group. Testing of eight selected compounds in the NCI 60-cell screen[18] yielded similar results. Triplicate tests of **1a**, **1c**, **3a**, **3c**, **4a**, **4b**, **4c**, and **4d** gave mean panel GI_{50} values (nM) of 4.9, 8.7, 686, 4 688, 6 098, >10 000, 3 833, and 8 391, respectively. GI_{50} compare correlations,[20] using **1a** as the seed against **1a**, **1c**, **3a**, **3c**, **4a**, **4b**, **4c**, and **4d**, were 1.00, 0.86, 0.84, <0.6, 0.74, <0.6, 0.62, and <0.6, respectively. The consistent inhibitory activity found for the (*S*,*S*)-diol (**4c**) compound compared to the (*R*,*R*)-diol (**4d**) chiral isomer provides another good illustration of the considerable differences in biological activity that can be expected for such enantiomeric pairs.

The diols **4c** and **4d** were also evaluated for potential inhibitory effects on tubulin polymerization, in comparison with combretastatin A-4 (**1c**). Consistent with its low cytotoxicity, diol **4d** was inactive as an inhibitor of tubulin assembly (IC_{50} value > 40 μM). In contrast, diol **4c** inhibited the reaction (IC_{50} 22 ± 0.9 (SD) μM), but it was much less potent than combretastatin A-4 (IC_{50} 1.2 ± 0.03 (SD) μM).

In contrast to the human cancer cell line results, the (1*S*,2*S*)- (**4a**) and (1*R*,2*R*)- (**4b**) diols were more microbiologically active than any derived compound (Table 3). With the exception of the Gram-negative pathogen *Neisseria gonorrhoeae*, the combretastatins show selectivity for Gram-positive bacteria (Table 3). With its abbreviated outer-membrane lipooligosaccharide, *N. gonorrhoeae* is more susceptible to hydrophobes than typical Gram-negative bacteria.

Experimental Section

The *trans*-stilbene silyl ether (**3c**) was synthesized as previously described.[18] 4-(Dimethylamino)pyridine, methanesulfonamide, *tert*-butyl alcohol, tetrabutylammonium fluoride, *p*-bromobenzoyl chloride, and AD mixes-α and -β were purchased from Sigma-Aldrich and used as received. Acetic anhydride was purchased from Acros and used as received. Pyridine and triethylamine were distilled and stored over KOH pellets. Methylene chloride (DCM) and DMF were distilled and stored over 4 Å molecular sieves. Organic extracts of aqueous workups were dried over magnesium sulfate. Solid samples and oils were dried under high vacuum (0.05 mmHg at 25 °C) unless otherwise noted. Flash column chromatography was performed on silica gel from EM Science (230−400 mesh).

Table 1. Physical Properties of the Diols and Derivatives

compd	yield (%)[a]	cryst solvent	mp (°C)	$[\alpha]^{25}_D$ (deg)	R_f values (hexanes−EtOAc)	formula analysis
4a	88	n/a	oil	−74.5 (*c*=0.68, $CHCl_3$)	0.18 (3:2)	($C_{24}H_{36}O_7Si$) C, H
4b	85	n/a	oil	+77.9 (*c*=0.42, $CHCl_3$)	0.18 (3:2)	($C_{24}H_{36}O_7Si$) C, H
4c	79	ether	89−90 (of hydrate)	−87.8 (*c*=0.32, MeOH)	0.07 (1:1)	($C_{18}H_{22}O_7 \cdot H_2O$) C, H
4d	77	ether	89−92 (of hydrate)	+89.7 (*c*=0.37, MeOH)	0.07 (1:1)	($C_{18}H_{22}O_7 \cdot H_2O$) C, H
4e	81	hexanes	90−92	−1.30 (*c*=0.77, $CHCl_3$)	0.14 (4:1)	($C_{28}H_{40}O_9Si$) C; H: calcd, 7.35; found, 7.80
4f	85	hexanes	89.5−90.5	+2.24 (*c*=1.3, $CHCl_3$)	0.14 (4:1)	($C_{28}H_{40}O_9Si$) C, H
4g	89	*b*	117−118	−59.3 (*c*=0.40, MeOH)	0.46 (2:1)	($C_{39}H_{31}O_{10}Br_3$) C, H, Br
4h	80	*b*	115−117	+60.9 (*c*=1.0, MeOH)	0.46 (2:1)	($C_{39}H_{31}O_{10}Br_3$) C, H
4i	93	EtOAc−hexanes	59−60	−65.9 (*c*=0.98, $CHCl_3$)	0.33 (4:1)	($C_{38}H_{42}O_9Br_2Si$) H, Br; C: calcd, 54.95; found, 55.51
4j	73	*b*	195−196 (of hydrate)	−57.5 (*c*=0.32, $CHCl_3$)	0.18 (2:1)	($C_{32}H_{28}Br_2O_9 \cdot 0.5H_2O$) C, H, Br
4k	79	carbon disulfide	70−72	+104.5 (*c*=0.22, $CHCl_3$)	0.18 (1:1)	($C_{25}H_{25}BrO_8$) C, H, Br
4l	91	*b*	68−70	+20.0 (*c*=0.30, $CHCl_3$)	0.60 (1:1)	($C_{29}H_{29}BrO_{10}$) C, H, Br

[a] Percent yield from starting material. [b] Crystallized following concentration of the flash column chromatography eluant.

Table 2. P388 Mouse Leukemia Cell Line (ED_{50}, μg/mL) and Human Tumor Cell Lines (GI_{50}, μg/mL)

	cell type											
compd	leukemia P388	ovarian OVCAR-3	CNS SF-295	renal A498	lung-NSC NCI−H460	colon KM20L2	melanoma SK-MEL-5	pancreas BXPC-3	pharynx FADU	neuroblast SK−N−SH	thyroid SW1736	prostate DU-145
1c	2.7×10^{-4}	$<1.0 \times 10^{-3}$	$<1.0 \times 10^{-3}$		5.6×10^{-4}	6.1×10^{-2}	2.0×10^{-4}	3.9×10^{-1}	6.5×10^{-4}	2.6×10^{-4}	7.1×10^{-4}	7.6×10^{-4}
2b	32.9				9.0			9.4	4.8	>10	>10	7.6
4c	2.0	0.38	0.52	0.91	2.5	0.52	0.70	3.9	0.60	0.28	1.8	2.1
4d	19.0	4.5	5.7	>10	4.4	8.2	4.9	>10	2.1	1.5	6.1	3.5

Table 3. Antimicrobial Activity of the Combretastatins

compd	microbe(s) inhibited	minimum inhibitory concentration (μg/disk)
1a	*N. gonorrhoeae*[9]	50−100
1b	*N. gonorrhoeae*	25−50
	S. aureus	50−100
1c	*N. gonorrhoeae*[18]	25−50
2c	*N. gonorrhoeae*	12.5−25
3a	*M. luteus*[9]	25−50
3c	*a*	
4a	*Str. pneumoniae*	25−50
4b	*Str. pneumoniae*	50−100
4c−4l	*a*	

[a] At 100 μg/disk no inhibition was observed.

Melting points were obtained using an Electrothermal 9100 apparatus and are uncorrected. TLC was performed with Analtech silica gel GHLF plates; all compounds were visible under short-wave UV light (254 nm) and stained with 2% ceric sulfate in ethanol. Mass spectra (FAB) were recorded using a Varian MAT 311A. ^{1}H NMR (300 MHz) was recorded on a Varian Gemini 300 instrument using deuterated chloroform as the solvent and referencing to TMS. ^{13}C NMR (100 MHz) was recorded on a Varian Gemini 400 instrument in $CDCl_3$. UV spectra were obtained employing a Perkin-Elmer Lambda 3B spectrometer interfaced with an IBM PC running PECSS data acquisition software or a UV−vis−NIR scanning spectrophotometer interfaced with a Shimadzu UV-3101PC. IR spectra were obtained with a Mattson 2020 Galaxy series FTIR instrument using NaCl plates. Combustion analyses were determined by the Galbraith Microanalytical Laboratory and are within ±0.3% of the calculated value. X-ray experiments were performed with an Enraf-Nonius CAD4 diffractometer.

Tubulin polymerization was evaluated as described previously.[20]

X-ray Crystal Structure Determination. Silyl ether of the *trans*-stilbene isomer, **3c**: Large, thick plates of the compound could be grown from hexane. A large crystal (~0.52 × 0.42 × 0.40 mm) of **3c** was used in the data collection, which was performed at 299 ± 1 K. Accurate cell dimensions were determined by least-squares fitting of 25 carefully centered reflections in the range of 35° < Θ < 40° using Cu Kα radiation.

Crystal data: $C_{24}H_{34}O_5Si_1$, FW = 430.60, orthorhombic, $P2_12_12_1$; a = 8.131(2), b = 9.441(1), c = 32.997(6) Å; V = 2533.0(8) Å^3, Z = 4, ρ_c = 1.129 Mg/M^3; μ(Cu Kα) = 1.053 mm^{-1}, λ = 1.54180 Å.

All reflections corresponding to more than a complete octant ($0 <= h <= 9$, $0 <= k <= 11$, $-3 <= l <= 38$) were collected over the range of 0 < 2Θ < 130° using the ω/2Θ scan technique. Three intensity control reflections were also measured for every 60 min of X-ray exposure time and showed a maximum variation of +4.7% over the course of the collection. Subsequent statistical analysis of the complete reflection data set using the XPREP[21] program, coupled with density measurements, verified that the space group was $P2_12_12_1$. After Lorentz and polarization corrections, merging of equivalent reflections, and rejection of systematic absences, 2 538 unique reflections (R(int) = 0.0311) remained, of which 2 385 were considered observed ($I_o > 2\sigma(I_o)$) and were used in the subsequent structure determination and refinement. Linear and anisotropic decay corrections were applied to the intensity data as well as an empirical absorption correction (based on a series of psi-scans).[22] Structure determination was readily accomplished with the direct-methods program SIR92.[23] All non-hydrogen atom coordinates were located in a routine run using default values in that program. The remaining H atom coordinates were calculated at optimum positions. All non-hydrogen atoms were refined anisotropically in a full-matrix least-squares refinement using SHELXL-97.[24] The H atoms were included; their U_{iso} thermal parameters were fixed at 1.2 the U_{iso} of the atom to which they were attached and forced to ride that atom. The final standard residual R_1 value for **3c** was 0.0624 for observed data and 0.0653 for all data. The goodness-of-fit on F^2 was 1.080. The corresponding Sheldrick R values were wR_2 of 0.1851 and 0.1892, respectively. A final difference Fourier map showed minimal residual electron density; the largest difference peak and hole being 0.891 and −0.385 e/Å^3, respectively. Final bond distances and angles were all within acceptable limits. The structure of the *trans*-isomer **3c** is shown in Figure 1.[25]

Asymmetric Dihydroxylation (4a, 4b): Representative Procedure. AD mix-α (8.4 g, 1.4 g/mmol of *trans*-stilbene silyl ether, **3c**) was added to a biphasic solution of butanol and water (30 mL each). After this dissolved, methanesulfonamide (0.57 g, 6.0 mmol, 1.0 equiv) was added, and the contents were cooled to 0 °C. The *trans*-silyl ether stilbene (**3c**) (2.6 g, 6.0 mmol, 1.0 equiv) was added and the reaction mixture stirred vigorously in the dark. After 24 h, additional AD mix-α (1.0 g) and another equivalent of methanesulfonamide were added. The contents were warmed to room temperature, and stirring continued until TLC (3:2 hexanes−EtOAc) showed no starting material (72 h total). Sodium sulfite (4 g) was added, 45 min later ethyl acetate (25 mL) was added, and the layers were separated. The aqueous layer was further washed with EtOAc (3 × 25 mL), the combined organic extracts were washed with 2 N KOH (50 mL), dried, and filtered, and solvent was removed in vacuo to give a yellow oil that was subjected to flash column chromatography (eluant 3:2 hexanes−EtOAc). Concentration of the desired fractions yielded **4a** as a clear oil: yield, 2.48 g; IR ν_{max} (Nujol) 3457w, 2955s, 2858s, 1593s, 1512s, 1462m, 1377m, 1236m, 1130m; ^{1}H NMR δ (300 MHz, $CDCl_3$) 0.07 (3H, s), 0.09 (3H, s), 0.96 (9H, s), 3.73 (6H, s), 3.76 (3H, s), 3.79 (3H, s), 4.55 (1H, d, J 7.7 Hz), 4.60 (1H, d, J 7.7 Hz), 6.33 (2H, s), 6.67 (1H, dd, J 2, 8.5 Hz), 6.72 (1H, s), 6.73 (1H, d, J 8.5 Hz); ^{13}C NMR δ (75 MHz, $CDCl_3$) 152.86, 150.79, 144.81, 137.40, 135.49, 132.62, 120.45, 119.73, 111.68, 103.91, 79.30, 78.75, 60.81, 56.00, 55.56, 25.69, 18.41, −4.73; EIMS m/z 464 (0.1%, M$^+$), 449 (1%, M$^+$ − CH_3), 407 (6%, M$^+$ − t-Bu), 267 (40%, M$^+$ − HOCH − $C_6H_2(OCH_3)_3$), 198 (100%, M$^+$ − HOCH − $C_6H_3(OCH_3)$(OTBDMS)).

Similarly, the resultant diol from AD mix-β gave **4b** as a clear oil (2.40 g): IR ν_{max} (Nujol) 3408w, 2924s, 2854s, 1593s, 1512s, 1462m, 1377m, 1236m, 1130m; ^{1}H NMR δ (300 MHz, $CDCl_3$) 0.07 (3H, s), 0.09 (3H, s), 0.96 (9H, s), 3.73 (6H, s), 3.76 (3H, s), 3.80 (3H, s), 4.55 (1H, d, J 7.7 Hz), 4.60 (1H, d, J 7.7 Hz), 6.33 (2H, s), 6.67 (1H, dd, J 2, 8.5 Hz), 6.72 (1H, s), 6.73 (1H, d, J 8.5 Hz); ^{13}C NMR δ (100 MHz, $CDCl_3$) 152.85, 150.76, 144.79, 137.40, 135.42, 132.52, 120.41, 119.67, 111.63, 103.84, 79.27, 78.73, 60.78, 55.98, 55.53, 25.66, 18.41, −4.74; EIMS m/z 464 (0.5%, M$^+$), 449 (0.5%, M$^+$ − CH_3), 407 (6%, M$^+$ − t-Bu), 267 (40%, M$^+$ − HOCH − $C_6H_2(OCH_3)_3$), 198 (100%, M$^+$ − HOCH − $C_6H_3(OCH_3)$(OTBDMS)).

(1*S*,2*S*)- and (1*R*,2*R*)-1-(3-Hydroxy-4-methoxyphenyl)-2-(3′,4′,5′-trimethoxyphenyl)-1,2-ethanediol (4c, 4d): Representative Procedure. The TBDMS-protected phenol **4b** (1.20 g, 2.59 mmol) from the AD mix-β was dissolved in THF (50 mL), and tetrabutylammonium fluoride (2.59 mL, 2.59 mmol, 1.0 M) was added to the solution. The solution was stirred under Ar and monitored by TLC (3:2 hexanes−EtOAc). After 30 min, ice (20 g) was added and the resultant solution extracted with EtOAc (100 mL). The organic layer was washed successively with water (50 mL) and brine (50 mL), dried, and filtered, and solvent was removed in vacuo to give a creamy white/yellow solid. Flash chromatography (eluant 1:1 DCM−EtOAc) resulted in isolation of a white amorphous solid (**4d**): yield, 0.75 g; IR ν_{max} (Nujol) 3457w, 2922, 2854s, 1589s; ^{1}H NMR δ (300 MHz, $CDCl_3$) 3.74 (6H, s), 3.81 (3H, s), 3.86 (3H, s), 4.57 (1H, d, J 7 Hz), 4.64 (1H, d, J 7 Hz), 5.58 (1H, s, broad), 6.36 (2H, s), 6.58 (1H, dd, J 2, 8 Hz), 6.72 (1H, d, J 8 Hz), 6.88 (1H, d, J 2 Hz); EIMS m/z 350 (10%, M$^+$), 332 (5%, M$^+$ − H_2O), 198 (100%, M$^+$ − HOCH − $C_6H_3(OCH_3)$(OH)).

Synthesis of the monohydrate (1*S*,2*S*)-enantiomer **4c** from **4a** gave a white powder after recrystallization: IR ν_{max} (Nujol) 3457w, 2922, 2854s, 1589s; ^{1}H NMR δ (300 MHz, $CDCl_3$) 3.74 (6H, s), 3.81 (3H, s), 3.86 (3H, s), 4.57 (1H, d, J 7 Hz), 4.63 (1H, d, J 7 Hz), 5.60 (1H, s, broad), 6.36 (2H, s), 6.57 (1H, dd,

J 2, 8 Hz), 6.72 (1H, d, *J* 8 Hz), 6.87 (1H, d, *J* 2 Hz); EIMS *m*/*z* 350 (1%, M^+), 332 (1%, $M^+ - H_2O$), 198 (100%, $M^+ -$ HOCH $- C_6H_3(OCH_3)(OH)$).

X-ray Crystal Structure Determination. 1-(3-Hydroxy-4-methoxyphenyl)-2-(3′,4′,5′-trimethoxyphenyl)-1,2-ethanediol, **4d**: Plate-shaped crystals of the monohydrate of this compound were grown from an ether solution. A crystal (~0.32 × 0.30 × 0.18 mm) of **4d** was used in the data collection, which was performed at 298 ± 1 K. Accurate cell dimensions were determined by least-squares fitting of 25 carefully centered reflections in the range of 35° < Θ < 40° using Cu Kα radiation.

Crystal data: $C_{18}H_{22}O_7 \cdot 1H_2O$, FW = 368.37, orthorhombic, $P2_12_12_1$; a = 6.1050(2), b = 13.677(3), c = 21.478(4) Å; V = 1793.4(5) Å^3, Z = 4, ρ_c = 1.364 Mg/m^3; μ(Cu Kα) = 0.907 mm^{-1}, λ = 1.54180 Å.

All reflections corresponding to slightly more than a complete octant ($0 <= h <= 7$, $0 <= k <= 16$, $-1 < l <= 25$) were collected over the range of $0 < 2\Theta < 130°$ using the $\omega/2\Theta$ scan technique. The Friedel reflections were also collected (whenever possible) immediately after each reflection. Three intensity control reflections were also measured for every 60 min of X-ray exposure time and showed a maximum variation of −7.7% over the course of the collection. Statistical analysis of the complete reflection data set using the XPREP[21] program, coupled with density measurements, verified the space group as $P2_12_12_1$. After Lorentz and polarization corrections, merging of equivalent reflections, and rejection of systematic absences, 2 992 independent reflections (R(int) =0.1019) remained, of which 2 899 were considered observed ($I_o > 2\sigma(I_o)$) and were used in the subsequent structure determination and refinement. Linear and anisotropic decay corrections were applied to the intensity data as well as an empirical absorption correction (based on a series of psi-scans).[22] Structure determination was readily accomplished with the direct-methods program SIR92.[23] All non-hydrogen atom coordinates were located in a routine run using default values in that program. The remaining H atom coordinates were either determined by difference maps or calculated at optimum positions. All non-hydrogen atoms were refined anisotropically in a full-matrix least-squares refinement using SHELXL-93.[26] The H atoms were included; their U_{iso} thermal parameters were fixed at 1.5 the U_{iso} of the atom to which they were attached and forced to ride that atom. The final standard residual R_1 value for **4d** was 0.0745 for observed data and 0.0757 for all data. The goodness-of-fit on F^2 was 0.973. The corresponding Sheldrick R values were wR_2 of 0.2079 and 0.2098, respectively. A final difference Fourier map showed minimal residual electron density; the largest difference peak and hole being +0.355 and −0.351 e/Å^3, respectively. The final bond distances and angles were all within acceptable limits. The absolute structure of **4d** could not be assigned with certainty, since the value of the Flack parameter (0.23) deviated significantly from 0.00 (indicative of the correct enantiomer) and exhibited a large esd (0.31). Consequently, the structure of the 1-(3-hydroxy-4-methoxyphenyl)-2-(3′,4′,5′-trimethoxyphenyl)-1,2-ethanediol monohydrate (**4d**), as shown in Figure 2,[25] represents one of the two possible enantiomeric configurations.

(1*S*,2*S*)- and (1*R*,2*R*)-1,2-Di(*p*-bromobenzoyloxy)-1-(3-[*p*-bromobenzoyloxy]-4-methoxyphenyl)-2-(3′,4′,5′-trimethoxyphenyl)ethane (4g, 4h): Representative Procedure. The asymmetric triol **4c** (0.5 g, 1.43, 1.0 equiv) was dissolved in 2:1 pyridine−DMF (10 and 5 mL, respectively) while under Ar, and *p*-bromobenzoyl chloride (1.92 g, 8.56 mmol, 6.0 equiv) was added. The resultant suspension was stirred for 2 h, when TLC analysis showed no residual starting material and a single product. Ice (20 g) was added, and the contents were filtered. The residue was taken up in ethyl acetate (50 mL) and washed successively with 1 M HCl, water, 10% sodium bicarbonate, water, and brine. The organic layer was dried and filtered, and removal of solvent gave a yellow solid that was subjected to flash chromatography (eluant 4:1 hexanes−EtOAc). Concentration of the desired fractions led to a white solid (**4g**): yield, 1.14 g; ^{1}H NMR δ (400 MHz, $CDCl_3$) 3.74 (6H, s), 3.76 (3H, s), 3.78 (3H, s), 6.29 (1H, d, *J* 9 Hz), 6.33 (1H, d, *J* 9 Hz), 6.42 (2H, s), 6.84 (1H, d, *J* 8 Hz), 6.99 (1H, dd, *J* 2, 8 Hz), 7.18 (1H, d, *J* 2 Hz), 7.54 (4H, d, *J* 8 Hz), 7.66 (2H, d, *J* 8 Hz), 7.87 (2H, d, *J* 8 Hz), 7.88 (2H, d, *J* 8 Hz), 8.03 (2H, d, *J* 8 Hz); EIMS *m*/*z* 900 (5%, M^+), 183 (100%, $[OCC_6H_4Br]^+$).

4h was prepared similarly: ^{1}H NMR δ (300 MHz, $CDCl_3$) 3.74 (6H, s), 3.76 (3H, s), 3.78 (3H, s), 6.29 (1H, d, *J* 9 Hz), 6.33 (1H, d, *J* 9 Hz), 6.42 (2H, s), 6.84 (1H, d, *J* 8 Hz), 6.99 (1H, dd, *J* 2, 8 Hz), 7.18 (1H, d, *J* 2 Hz), 7.54 (4H, d, *J* 8 Hz), 7.66 (2H, d, *J* 8 Hz), 7.87 (2H, d, *J* 8 Hz), 7.88 (2H, d, *J* 8 Hz), 8.03 (2H, d, *J* 8 Hz); EIMS *m*/*z* 900 (5%, M^+), 183 (100%, $[OCC_6H_4Br]^+$).

(1*S*,2*S*)- and (1*R*,2*R*)-1,2-Diacetoxy-1-(3-[*tert*-butyldimethylsilyloxy]-4-methoxyphenyl)-2-(3′,4′,5′-trimethoxyphenyl)ethane (4e, 4f): Representative Procedure. Acetic anhydride (0.51 mL, 5.38 mmol, 2.5 equiv) was added to a solution of the diol (1.0 g, 2.15 mmol, 1.0 equiv) with triethylamine (0.90 mL, 6.46 mmol, 3.0 equiv) and DMAP (53 mg, 0.043 mmol, 0.2 equiv) in DCM (5 mL) under Ar at room temperature. The yellow solution was stirred for 50 min, and TLC (3:2 hexanes−EtOAc) showed no residual starting material. Methanol (5 mL) was added and the reaction mixture concentrated to a yellow oil that was washed with ether (10 mL) and evaporated. The oil was partitioned with ether (25 mL) and 1 N HCl (25 mL). The organic layer was further washed with 10% aqueous sodium bicarbonate (25 mL) and water (25 mL) and dried. Filtration followed by removal of solvent in vacuo gave rise to a yellow oil that was subjected to flash column chromatography (4:1 hexanes−EtOAc). The desired fractions were concentrated to a clear oil which crystallized upon standing: yield, 0.95 g. **4e**: ^{1}H NMR δ (300 MHz, $CDCl_3$) 0.04 (3H, s), 0.07 (3H, s), 0.95 (9H, s), 2.09 (3H, s), 2.10 (3H, s), 3.73 (6H, s), 3.74 (3H, s), 3.78 (3H, s), 5.90 (1H, d, *J* 9 Hz), 5.93 (1H, d, *J* 9 Hz), 6.33 (2H, s), 6.68 (3H, m); EIMS *m*/*z* 548 (10%, M^+), 491 (70%, $M^+ - t$-Bu), 267 (100%, $M^+ -$ AcOCHC$_6$H$_2$(OCH$_3$)$_3$ − Ac), 197 (80%, $M^+ -$ AcOCHC$_6$H$_3$-(OCH$_3$)(OTBDMS) − Ac).

4f was isolated as large glassy cubes: ^{1}H NMR δ (300 MHz, $CDCl_3$) 0.04 (3H, s), 0.07 (3H, s), 0.95 (9H, s), 2.09 (3H, s), 2.10 (3H, s), 3.73 (6H, s), 3.74 (3H, s), 3.78 (3H, s), 5.90 (1H, d, J 9 Hz), 5.93 (1H, d, *J* 9 Hz), 6.33 (2H, s), 6.68 (3H, m); EIMS *m*/*z* 548 (5%, M^+), 491 (60%, $M^+ - t$-Bu), 267 (100%, $M^+ -$ AcOCHC$_6$H$_2$(OCH$_3$)$_3$ − Ac), 197 (80%, $M^+ -$ AcOCHC$_6$H$_3$-(OCH$_3$)(OTBDMS) − Ac).

X-ray Crystal Structure Determination. *tert*-Butyldimethylsilyl diacetate derivative, **4e**: Large, thick plates of the compound were grown from hexane. A large crystal (~0.52 × 0.44 × 0.40 mm) of **4e** was used in the data collection, which was performed at 296 ± 1 K. Accurate cell dimensions were determined by least-squares fitting of 25 carefully centered reflections in the range of 35° < Θ < 40° using Cu Kα radiation.

Crystal data: $C_{56}H_{80}O_{18}Si_2$, FW = 1087.38, triclinic, $P\bar{1}$; a = 9.103(5), b = 12.782(5), c = 14.164(5) Å; α = 111.29(2), β = 97.92(2), γ = 91.00(2); V = 1516.8(12) Å, Z = 1, ρ_c = 1.201 Mg/m^3; μ(Cu Kα) = 1.088 mm^{-1}, λ = 1.54180 Å.

All reflections corresponding to a complete hemisphere ($0 <= h <= 10$, $-15 <= k <= 15$, $-16 <= l <= 16$) were collected over the range of $0 < 2\Theta < 130°$ using the $\omega/2\Theta$ scan technique. The Friedel reflections were also collected (whenever possible) immediately after each reflection. Three intensity control reflections were also measured for every 60 min of X-ray exposure time and showed a maximum variation of +6.2% over the course of the collection. Subsequent statistical analysis of the complete reflection data set using the XPREP[21] program verified the space group as $P\bar{1}$, with two independent molecules in the asymmetric unit cell. After Lorentz and polarization corrections, merging of equivalent reflections, and rejection of systematic absences, 10 168 unique reflections (R(int)=0.0447) remained, of which 9 928 were considered observed ($I_o > 2\sigma(I_o)$) and were used in the subsequent structure determination and refinement. Linear and anisotropic decay corrections were applied to the intensity data as well as an empirical absorption correction (based on a series

of psi-scans).[22] Structure determination was readily accomplished with the direct-methods program SIR92.[23] All nonhydrogen atom coordinates were located in a routine run using default values in that program. The remaining H atom coordinates were calculated at optimum positions. All nonhydrogen atoms were refined anistropically in a full-matrix least-squares refinement using SHELXL-97.[24] The H atoms were included; their U_{iso} thermal parameters were fixed at 1.5 the U_{iso} of the atom to which they were attached and forced to ride that atom. The final standard residual R_1 value for **4e** was 0.0634 for observed data and 0.0642 for all data. The goodness-of-fit on F^2 was 1.036. The corresponding Sheldrick R values were wR_2 of 0.1726 and 0.1732, respectively. A final difference Fourier map showed minimal residual electron density; the largest difference peak and hole being 0.280 and −0.163 e/Å^3, respectively. The absolute structure of **4e** could be assigned with certainty based on the value of the Flack parameter (0.06, esd 0.03) for the enantiomer shown in Figure 3.[25] Consequently, the absolute stereochemistry of structure of the silyl-protected diacetate derivative **4d** can be assigned the *S* configuration at both chiral carbons, C1A and C1′A. Final bond distances and angles were all within acceptable limits.

(1*S*,2*S*)-1,2-Di(*p*-bromobenzoyloxy)-1-(3-[*tert*-butyldimethylsilyloxy]-4-methoxyphenyl)-2-(3′,4′,5′-trimethoxyphenyl)ethane (4i). The resultant diol from AD mix-α **4a** (0.75 g, 1.61 mmol, 1.0 equiv) was dissolved in DMF (15 mL), and pyridine (15 mL, 1:1 DMF−pyridine) was added at room temperature. The reaction was stirred until homogeneous, and 4-bromobenzoyl chloride (0.89 g, 4.04 mmol, 2.5 equiv) was added all at once. The yellow mixture was stirred under Ar at room temperature. A white precipitate formed within 30 min, and after 2 h the temperature was raised to 45 °C; 16 h later, the temperature was raised to 85 °C, and another 2.5 equiv of 4-bromobenzoyl chloride was added. No starting material was visualized following TLC. Ice (30 g) and ether (25 mL) were added. The ethereal layer was successively washed with 1 M HCl (25 mL), 10% sodium bicarbonate (25 mL), and water (25 mL). The organic phase was dried and filtered, and solvent was removed to give a yellow oil that was subjected to flash chromatography (9:1 hexanes−EtOAc). The desired product (R_f = 0.33, 4:1 hexanes−EtOAc) was isolated as an off-white solid that was recrystallized from EtOAc−hexane to afford small needles: yield, 0.70 g; ^{1}H NMR δ (300 MHz, $CDCl_3$) −0.02 (3H, s), 0.04 (3H, s), 0.92 (9H, s), 3.70 (6H, s), 3.73 (3H, s), 3.76 (3H, s), 6.23 (1H, d, *J* 9 Hz), 6.29 (1H, d, *J* 9 Hz), 6.41 (2H, s), 6.70 (1H, d, *J* 8 Hz), 6.78 (1H, s), 6.79 (1H, d, *J* 8 Hz), 7.52 (4H, d, *J* 8 Hz), 7.84 (4H, d, *J* 8 Hz); EIMS *m*/*z* 830 (2%, M^+2), 828 (1%, M^+), 774 (15%, $M^+ - t$-Bu + H), 183 (100%, $[OCC_6H_4Br]^+$).

(1*S*,2*S*)-1,2-Di(*p*-bromobenzoyloxy)-1-(3-hydroxy-4-methoxyphenyl)-2-(3′,4′,5′-trimethoxyphenyl)ethane (4j). **4i** (1.24 g, 1.49 mmol) was converted to **4j** in an identical fashion to the deprotection procedure of **4c**. After flash chromatography (2:1 hexanes−EtOAc), the desired fractions were concentrated to give a fine woolly solid (**4j**): yield, 0.79 g; ^{1}H NMR δ (400 MHz, $CDCl_3$) 3.72 (6H, s), 3.78 (3H, s), 3.84 (3H, s), 5.56 (1H, s), 6.29 (1H, d, *J* 9 Hz), 6.29 (1H, d, *J* 9 Hz), 6.43 (2H, s), 6.67 (1H, dd, *J* 2, 8 Hz), 6.68 (1H, d, *J* 8 Hz), 6.97 (1H, d, *J* 2 Hz), 7.54 (4H, m), 7.87 (4H, m); EIMS *m*/*z* 716 (10%, M^+), 516 (5%, $M^+ - HO_2CC_6H_4Br$), 183 (100%, $[OCC_6H_4Br]^+$).

(1*R*,2*R*)-1,2-Dihydroxy-1-(3-[*p*-bromobenzoyloxy]-4-methoxyphenyl)-2-(3′,4′,5′-trimethoxyphenyl)ethane (4k). The chiral phenol **4d** (0.5 g, 1.43 mmol, 1.0 equiv) was dissolved in DMF (20 mL), and triethylamine (0.40 mL, 2.85 mmol, 2.0 equiv) was added. After 10 min, addition of *p*-bromobenzoyl chloride (0.31 g, 1.43 mmol, 1.0 equiv) resulted in a yellow solution as the reaction proceeded at room temperature under Ar. Starting material could no longer be visualized by TLC after 2 h. Ice was added, and a precipitate formed that was removed by filtration. The aqueous filtrate was washed with ethyl acetate (25 mL), and the concentrated residue was added to the filtered solid and flash chromatographed (1:1 hexanes−EtOAc). The desired fraction were concentrated, yielding a white solid. This was recrystallized from carbon disulfide to give a white powder: yield, 0.60 g; ^{1}H NMR δ (300 MHz, $CDCl_3$) 3.70 (6H, s), 3.72 (3H, s), 3.75 (3H, s), 4.54 (2H, s (coalesced doublet)), 6.29 (2H, s), 6.78 (1H, d, *J* 8 Hz), 6.83 (1H, dd, *J* 2, 8 Hz), 7.03 (1H, d, *J* 2 Hz), 7.61 (2H, d, *J* 8 Hz), 8.00 (2H, d, *J* 8 Hz); EIMS *m*/*z* 532 (1%, M^+), 517 (5%, $M^+ - CH_3$), 514 (5%, $M^+ - H_2O$), 335 (5%, $M^+ - OCH - C_6H_3(OCH_3)_3$), 198 (100%, $M^+ - HOCH - C_6H_3(OCH_3)$-$(O_2C_6H_4Br)$), 183 (45%, $[OCC_6H_4Br]^+$).

(1*R*,2*R*)-1,2-Diacetoxy-1-(3-[*p*-bromobenzoyloxy]-4-methoxyphenyl)-2-(3′,4′,5′-trimethoxyphenyl)ethane (4l). Acetic anhydride (84 μL, 0.89 mmol, 2.5 equiv) was added to a solution of the diol **4k** (0.19 g, 0.36 mmol, 1.0 equiv) with DMAP (8.8 mg, 0.071 mmol, 0.2 equiv) and triethylamine (0.15 mL, 1.07 mmol, 3.0 equiv) in DCM (1 mL) under Ar at room temperature. The contents were stirred for 3 h, and TLC (1:1 hexanes−EtOAc) showed no residual starting material. Methanol (5 mL) was added and the reaction mixture concentrated to a yellow oil that was washed with ether, which was removed by evaporation. The oily residue was partitioned with ether (15 mL) and 1 N HCl (15 mL). The organic layer was further washed with 10% aqueous sodium bicarbonate (15 mL). The combined aqueous layers were back-extracted with DCM (5 mL), and the organic layers were combined and dried. Filtration and evaporation of solvents gave an off-white solid that was subjected to flash chromatography (eluant 1:1 hexanes−EtOAc). The desired fractions were collected and concentrated, producing a white solid: yield, 0.20 g; ^{1}H NMR δ (300 MHz, $CDCl_3$) 2.10 (3H, s), 2.12 (3H, s), 3.75 (3H, s), 3.76 (6H, s), 3.78 (3H, s), 5.93 (1H, d, *J* 9 Hz), 5.97 (1H, d, *J* 9 Hz), 6.34 (2H, s), 6.80 (1H, d, *J* 8 Hz), 6.89 (1H, dd, *J* 2, 8 Hz), 7.08 (1H, d, *J* 2 Hz), 7.65 (2H, d, *J* 8 Hz), 8.03 (2H, d, *J* 8 Hz); EIMS *m*/*z* 616 (15%, M^+), 559 (1%, $M^+ - O_2CCH_3$), 498 (5%, $M^+ - (O_2CCH_3)_2$), 434 (6%, M + H − OCC_6H_4Br), 197 (100%, $[HOCHC_6H_2(OCH_3)_3]^+$), 183 (55%, $[OCC_6H_4Br]^+$).

Antimicrobial Susceptibility Testing. Compounds were screened against the bacteria *Stenotrophomonas maltophilia*, *Micrococcus luteus*, *Staphylococcus aureus*, *Escherichia coli*, *Enterobacter cloacae*, *Enterococcus faecalis*, *Streptococcus pneumoniae*, and *Neisseria gonorrhoeae* and the fungi *Candida albicans* and *Cryptococcus neoformans*, according to established disk susceptibility testing protocols.[27]

Acknowledgment. Appreciation and thanks for support of this research are extended to Outstanding Investigator Grant CA 44344-05-9 with the Division of Cancer Treatment and Diagnosis, NCI, DHHS, the Arizona Disease Control Research Commission, Virginia Piper, Diane Cummings Halle, Gary L. and Diane R. Tooker, Polly Trautman, John and Edith Reyno, the Caitlin Robb Foundation, and the Robert B. Dalton Endowment. We also thank Drs. Cherry L. Herald, Fiona Hogan, Jean M. Schmidt, and Michael D. Williams, as well as David M. Carnell, Laura Crews, and Lee Williams, the National Science Foundation for equipment Grant CHE-8409644, and the NSF Regional Instrumentation Facility in Nebraska (Grant CHE-8620177).

Supporting Information Available: Expanded Table 2 containing the murine P388 and human cancer cell line results for the less active and inactive compounds **4a**, **4b**, and **4g**−**4l**; X-ray crystallographic tables of experimental detail, atomic coordinates, bond lengths and angles, and anisotropic thermal parameters for **3c**, **4d**, and **4e**. This information is available free of charge via the Internet at http://pubs.acs.org.

References

(1) For contribution 409, refer to: Pettit, G. R.; Tan, R.; Melody, N.; Kielty, J. M.; Pettit, R. K.; Herald, D. L.; Tucker, B.; Mallavia, L. P.; Doubek, D. L.; Schmidt, J. M. Antineoplastic Agents 409. Isolation and Structure of Montanastatin from a Terrestrial Actinomycete. *Bioorg. Med. Chem.*, in press.

(2) Weidner, N.; Folkman, J. Tumor Vascularity as a Prognostic Factor in Cancer. In *Cancer: Principles & Practice of Oncology Updates*; DeVita, V. T., Hellman, S., Rosenberg, S. A., Eds.; J. B. Lippincott: Philadelphia, 1997; Vol. 11, pp 1−24.
(3) Pluda, J. M. Tumor-Associated Angiogenesis: Mechanisms, Clinical Implications, and Therapeutic Strategies. *Semin. Oncol.* **1997**, *24*, 203−218.
(4) Folkman, J. New Perspectives in Clinical Oncology from Angiogenesis Research. *Eur. J. Cancer* **1996**, *32A*, 2534−2539.
(5) D′Amato, R. J.; Loughnan, M. S.; Flynn, E.; Folkman, J. Thalidomide is an Inhibitor of Angiogenesis. *Proc. Natl. Acad. Sci. U.S.A.* **1994**, *91*, 4082−8085.
(6) Sin, N.; Meng, L.; Wang, M. Q. W.; Wen, J. J.; Bornmann, W. G.; Crews, C. M. The Anti-angiogenic Agent Fumagillin Covalently Binds and Inhibits the Methionine Aminopeptidase, MetAP-2. *Proc. Natl. Acad. Sci. U.S.A.* **1997**, *94*, 6099−6103.
(7) Dark, G. G.; Hill, S. A.; Prise, V. E.; Tozer, G. M.; Pettit, G. R.; Chaplin, D. J. Combretastatin A-4, an Agent That Displays Potent and Selective Toxicity Toward Tumor Vasculature. *Cancer Res.* **1997**, *57*, 1829−1834.
(8) Pettit, G. R.; Smith, C. R.; Singh, S. B. Recent Advances in the Chemistry of Plant Antineoplastic Constituents. In *Biologically Active Natural Products*; Hostettmann, K., Lea, P. J., Eds.; Clarendon Press: Oxford, 1987; pp 105−116.
(9) Pettit, G. R.; Rhodes, M. R.; Herald, D. L.; Chaplin, D. J.; Stratford, M.; Pettit, R. K.; Chapuis, J.-C.; Oliva, D.; Hamel, E. Antineoplastic Agents 393. Synthesis of the *trans*-Isomer of Combretastatin A-4 Prodrug. *Anti-Cancer Drug Des*., in press.
(10) Bedford, S. B.; Quarterman, C. P.; Rathbone, D. L.; Slack, J. A.; Griffin, R. J.; Stevens, M. F. G. Synthesis of Water-soluble Prodrugs of the Cytotoxic Agent Combretastatin A-4. *BioMed. Chem. Lett.* **1996**, *6*, 157−160.
(11) Jang, M.; Cai, L.; Udeani, G. R.; Slowing, K. V.; Thomas, C. F.; Beecher, C. W. W.; Fong, H. H. S.; Farnsworth, N. R.; Kinghorn, A. D.; Mehta, R. G.; Moon, R. C.; Pezzuto, J. M. Cancer Chemopreventive Activity of Resveratrol, a Natural Product Derived from Grapes. *Science* **1997**, *275*, 218−220.
(12) Teguo, P. W.; Decendit, A.; Krisa, S.; Deffieux, G.; Vercauteren, J.; Mérillon, J.-M. The Accumulation of Stilbene Glycosides in *Vitis vinifera* Cell Suspension Cultures. *J. Nat. Prod.* **1996**, *59*, 1189−1191.
(13) Bishop, A. C.; Moore, D.; Scanlan, T. S.; Shokat, K. M. Screening a Hydroxystilbene Library for Selective Inhibition of the B Cell Antigen Receptor Kinase Cascade. *Tetrahedron* **1997**, *53*, 11995−12004.
(14) Chen, K.; Kuo, S.-C.; Hsieh, M.-C.; Mauger, A.; Lin, C. M.; Hamel, E.; Lee, K.-H. Antitumor Agents. 178. Synthesis and Biological Evanuation of Substituted 2-Aryl-1,8-naphthyridin-4(1*H*)-ones as Antitumor Agents that Inhibit Tubulin Polymerization. *J. Med. Chem.* **1997**, *40*, 3049−3056.
(15) Cushman, M.; He, H.-M.; Katzenellenbogen, J. A.; Varma, R. K.; Hamel, E.; Lin, C. M.; Ram, S.; Sachdeya, Y. P. Synthesis of Analogues of 2-Methoxyestradiol with Enhanced Inhibitory Effects on Tubulin Polymerization and Cancer Cell Growth. *J. Med. Chem.* **1997**, *40*, 2323−2334.
(16) Mannila, E.; Talvitie, A. Combretastatin Analogues via Hydration of Stilbene Derivatives. *Liebigs Ann. Chem.* **1993**, 1037−1039.
(17) Medarde, M.; Peláez-Lamamié de Clairac, Ramos, A. C.; Caballero, E.; López, J. L.; Grávalos, D. G.; Feliciano, A. S. Synthesis and Pharmacological Activity of Combretastatin Analogues, Naphthylcombretastatins and Related Compounds. *BioMed. Chem. Lett.* **1995**, *5*, 229−232.
(18) Pettit, G. R.; Singh, S. B.; Boyd, M. R.; Hamel, E.; Pettit, R. K.; Schmidt, J. M.; Hogan, F. Antineoplastic Agents 291. Isolation and Synthesis of Combretastatins A-4, A-5, and A-6. *J. Med. Chem.* **1995**, *38*, 1666−1672.
(19) Pettit, G. R.; Singh, S. B.; Niven, M. L.; Hamel, E.; Schmidt, J. M. Isolation, Structure, and Synthesis of Combretastatins A-1 and B-1, Potent New Inhibitors of Microtubule Assembly, Derived from *Combretum caffrum*. *J. Nat. Prod.* **1987**, *50*, 119−131.
(20) Pettit, G. R.; Toki, B.; Herald, D. L.; Verdier-Pinard, P.; Boyd, M. R.; Hamel, E.; Pettit, R. K. Antineoplastic Agents 379. Synthesis of Phenstatin Phosphate. *J. Med. Chem.* **1998**, *41*, 1688−1695.
(21) XPREP—The automatic space group determination program in the SHELXTL PC program package (see ref 25).
(22) North, A. C. T.; Phillips, D. C.; Mathews, F. S. *Acta Crystallogr.* **1968**, *A24*, 351−359.
(23) Altomare, A.; Cascarano, G.; Giacovazzo, C.; Guagliardi, A.; Burla, M.; Polidori, G.; Camalli, M. SIR92 − A Program for Automatic Solution of Crystal Structures by Direct Methods; Dipartimento Geomineralogico, University of Bari: Bari, Italy.
(24) Sheldrick, G. M. SHELXL-97. Crystal Structure Refinement − DOS/WIN95/NT Version, Release 97-2; Institut Anorg. Chemie: Göttingen, Germany, 1998.
(25) Preparation of Figures 1−3 was done with SHELXTL-PC version 5.03, 1994, an integrated software system for the determination of crystal structures from diffraction data; Siemens Industrial Automation, Inc., Analytical Instrumenation, Madison, WI 53719.
(26) Sheldrick, G. M. SHELXL93. Program for the Refinement of Crystal Structures; Institut Anorg. Chemie: Göttingen, Germany, 1993.
(27) National Committee for Clinical Laboratory Standards. 1997. *Performance standards for antimicrobial disk susceptibility tests*, 6th ed.; approved standard M2-A6; NCCLS: Wayne, PA.

JM9807149